


RESEARCH

Open Access



Wind tunnel test on low-rise buildings influenced by hillside height in typical mountain terrain

Min Zhong^{1,2,3}, Minghui Lin², Zhanxue Zhou^{2*} , Zhengnong Li³, Junyu Lu² and Fen Xu¹

*Correspondence:
zhanxuez@163.com

¹ Jiangsu Open University,
Nanjing 210000, China

² Hebei University of Architecture,
Zhangjiakou 075132, China

³ Hunan University,
Changsha 410082, China

Abstract

Hills and mountain fields have a high proportion in coastal areas around the world. Especially in China, lots of low-rise buildings are in complex mountain terrain. Compared with the flat topography under typhoons, due to the change caused by complex topography, the damage ratio of low-rise buildings is much larger. This paper investigates the wind pressure distribution in three different configurations of typical mountain terrain on low-rise buildings in coastal areas by wind tunnel tests. At the same time, the results are compared with the wind pressure distribution of low-rise buildings without surrounding structures. The variation of the average pressure coefficient and shape coefficient with the change of hillside height under a wind attack angle of 0° and the trends of average wind pressure coefficients of a low-rise building under wind attack angles of 0°–90° are studied. The results show that the distribution of pressure in low buildings is significantly affected by the height of the mountain. When the hillside height is half of the scale physical model, the influence coefficient from the mountain to each surface of the whole building is within 50%. When the hillside height is four times that of the model, the influence factor from the mountain to each surface of the whole building is obvious and is most significantly influenced by the leeward roof. The mean design criteria of the low-rise building, such as windward midline, leeward roof, and windward roof in these three typical mountain terrains, should be designed for their higher absolute value of the average pressure coefficient. The mean pressure coefficient under different wind angles and mountain environments has a significant relationship. The most unfavorable wind angle of wind load calculations should be considered when designing low-rise buildings.

Keywords: Low-rise buildings, Mountain terrain, Wind load, Wind tunnel experiment, Pressure coefficient

1 Introduction

Hills and mountain fields have a high proportion in coastal areas around the world. Especially in China, lots of low-rise buildings are in complex mountain terrain. Compared with the flat topography under typhoons, due to the change caused by complex topography, the damage ratio of low-rise buildings is much larger. Low-rise buildings always suffer from the threats of typhoons due to their special location and terrain. Unfortunately,

Chinese scholars have not paid much attention to the impacts of wind pressure on low-rise buildings, and few experiments have been conducted on the interference effects of wind tunnels on low buildings in typical mountainous landscapes. Isolated low-rise buildings have received much attention, and there is a well-established understanding of the mechanism of mean and fluctuating forces on them. John et al. [1] discussed a wind tunnel study of wind loads on a gable roof building with the interference of a boundary wall. The paper provided information regarding pressure variations on the overhang, roof, and wall surface of a gable roof building due to the interference effect of a boundary wall. It has been found that pressure coefficients change significantly on both roofs and walls of buildings in the presence of boundary walls placed at varying distances. At the same time, Lien et al. [2] and Zhang et al. [3] simulated the flow patterns for different building arrangements to validate the numerical modeling and to investigate the effect of surrounding buildings, pointing out that upstream buildings significantly affect wind loads and flow patterns on the target building. The interference effect on the distance between low-rise buildings and their surrounding buildings has been studied. Holmes [4] studied the effect of building groups in characteristic suburban street patterns. It was found that a significant increase in the magnitude of the negative roof pressure occurs when one extra row of houses is added to each side of an isolated low-rise building. The shielding effect of upwind buildings depends strongly on the ratio of the building's spacing to height. Pindado et al. [5] analyzed a low-rise building model with a flat roof equipped with pressure taps on the roof and different block-type buildings, but the paper only figured out whether the upstream building was the same high or higher than the downstream one. The relationships between the interference effects and the height of surrounding buildings have been studied. Experimental results revealed that the wind load increases as the relative height of the upstream building increases. The wind load is the highest for intermediate distances between buildings when a passage between these buildings is formed. Many papers have also shown the interference effects of low-rise buildings located among a large group of surrounding buildings. Tsutsumi et al. [6] studied the interaction of regularly arranged buildings. Kim et al. [7] conducted systematic wind pressure measurements to investigate the effect of a large group of surrounding buildings on wind pressures in a typical low-rise building. The primary purpose of this work was to understand and quantify the effects of nearby structures on engineers, especially concerning maximum and minimum values. Chang and Meroney [8] investigated the sensitivity of these high suction to the presence of multiple surrounding building configurations. This study used the Wind Engineering Research Field Laboratory building for study during the CSU/TTU Cooperative Program in Wind Engineering as a basic building shape. A physical on-scale model of the WERFL structure was constructed and instrumented with multiple pressure ports. Kim et al. [9] conducted wind tunnel tests on low-rise buildings with flat roofs, and the study showed that the construction form and height of the parapet wall affected the wind load and pressure characteristics of the roof. Cantilevers are prone to damage during wind disasters. Mostafa et al. [10] conducted large-scale experiments using two models and confirmed that the width of the cantilever had a significant impact on local wind pressure changes. Based on the assumption that aerodynamics and statics can be separated, Kopp and Wu [11] proposed a framework to compare the differences between building models in tornado wind fields and boundary

layer wind tunnels. The research results show that the curvature of tornado wind fields affects the magnitude of the differences. Zhong et al. [12, 13] studied the variation of the average pressure coefficient and shape coefficient with the change of hillside slope under a wind attack angle of 0° . The trends of average wind pressure coefficients of low-rise buildings under wind attack angles of $0^\circ - 90^\circ$ were analyzed. It was found that the pressure distribution of low-rise buildings is significantly affected by the slope of the mountain, especially the leeward side. The wind pressure distribution of low-rise buildings under hillside terrain is relatively complex. Current research only studies the wind resistance performance of low-rise buildings under different slopes and spacing but does not study the law of the influence of hillside height on wind pressure. Since the height of the hill has a relatively large impact on the flow field distribution around low-rise buildings, it is necessary to study the influence law of wind pressure distribution with hillside height. This study will provide a theoretical basis for the wind-resistant design of low-rise buildings in mountainous terrain.

In this paper, wind tunnel tests are carried out to investigate the effect of wind pressure on low-rise buildings in typical mountain terrain. A relationship of mean pressure coefficient between different wind angles and mountain environments is found. It is suggested that the influence of the most unfavorable wind angle on the wind pressure should be considered in the wind-resistant design of low-rise buildings.

2 Wind tunnel test experiments

Wind tunnel test experiments are carried out in the boundary layer of wind tunnel test equipment in the Department of Civil Engineering, Hunan University, China. The working section is 3.0 meters wide, 2.5 meters high, and 10 meters long.

2.1 Introduction of wind tunnel model and measuring point arrangement

The atmospheric boundary layer is simulated as a geometrical scale of 1:40. As shown in Fig. 1, the physical on-scale model of the building is designed based on the most common low-rise buildings in China. The size of the physical on-scale mountain model is based on the “Load code for the design of building structures (GB 50009–2012)”, which encloses the design of gable roofs in low-rise buildings near a mountain.

The physical on-scale building model (geometric scale of 1:40) is fabricated to represent a building with a height (H) of 6.83 m, a width (W) of 4.45 m, and a length (L) of 7.5 m — the roof with an overhang extended up to 0.25 m from the building wall. The pressure tap testing points are located at all four external walls, the roof, and double sides of the eaves. There are 374 pressure tap testing points in total, with 202 testing points on the walls, 130 testing points on the roof, and 42 testing points inside the eaves. The detailed arrangement of the pressure tap testing points are shown in Fig. 2.

2.2 Experimental operating conditions

Figure 3 shows the location of the low-rise building and the typical mountain terrain. H is the total height of the low-rise building; H_m is the hillside height; β is the angle between the ground and the hillside; α is the roof angle; S is the distance between the hillside and the low-rise building. The experiment is performed under the angle of wind attack from 0° to 90° with an interval of 5° , as shown in Fig. 4. The physical

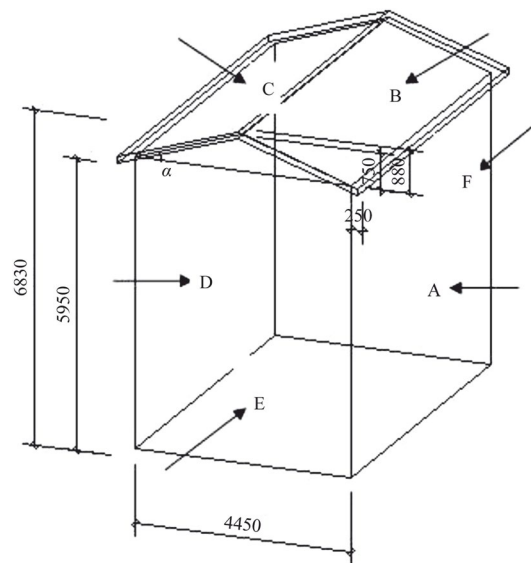


Fig. 1 Physical on-scale low-rise building model (units: mm)

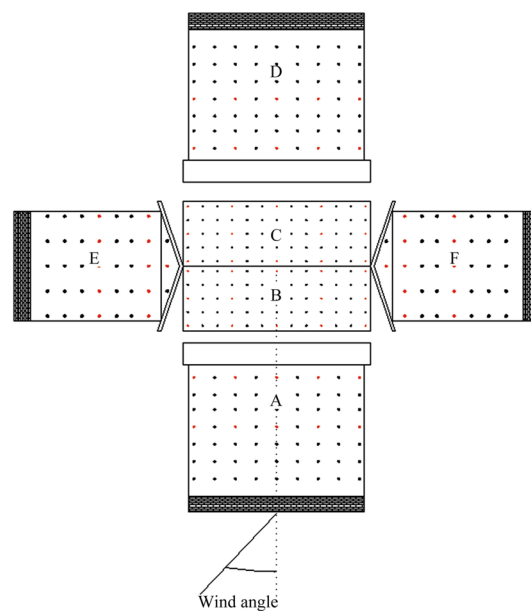


Fig. 2 Detail of the pressure tap testing points

on-scale model of the building used for the wind tunnel test is in the northern direction when the wind direction is 0° . To find out how the wind pressure is affected by the hillside height directly, the hillside without the surrounding area is set. A series of wind tunnel experiment parameters for the ratio of hillside height to low-rise building height are selected to study. Details of the parameters are shown in Table 1. The wind tunnel test conditions satisfy all the relevant requirements of the blocking probability.

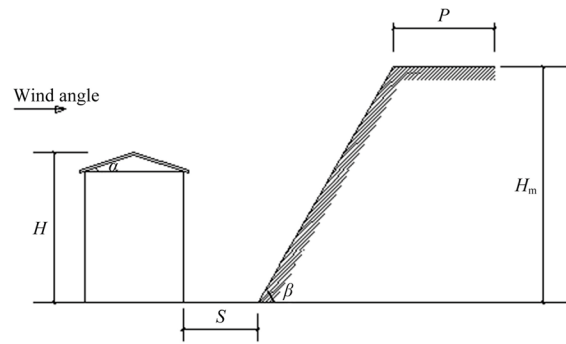


Fig. 3 Position of the mountain

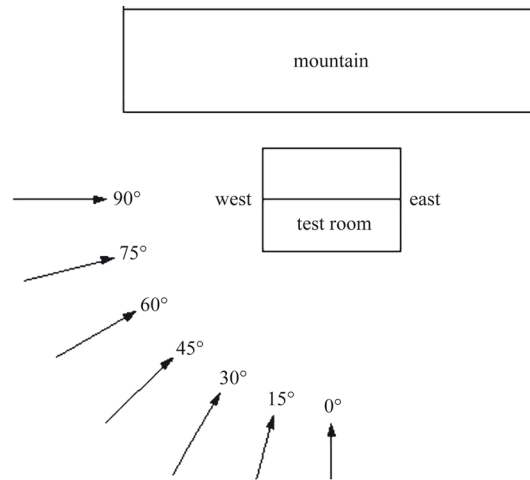


Fig. 4 Wind direction

Table 1 Experimental parameter study detail

Model dimensions	Plan dimensions	111.25 mm (width) × 187.5 mm (length)
	Eave height	148.75 mm
	Roof height	170.75 mm
	Roof slope	18.6°
Position of the mountain	Distance between the mountain and the model	34.15 mm ($S/H=0.2$)
	Mountain height H_m	8.5375 mm ($H_m/H=0.5$) 34.15 mm ($H_m/H=2$) 68.3 mm ($H_m/H=4$)
	Slope of the mountain, β	60°
Terrain roughness, z_0	0.12	
Wind angles	0° – 90° (5° increments)	
Number of taps	374	
Sampling frequency	312.5 Hz	
Reference wind tunnel speed	12 m/s	
Model length scale	1:40	



Fig. 5 Experimental models in the wind tunnel

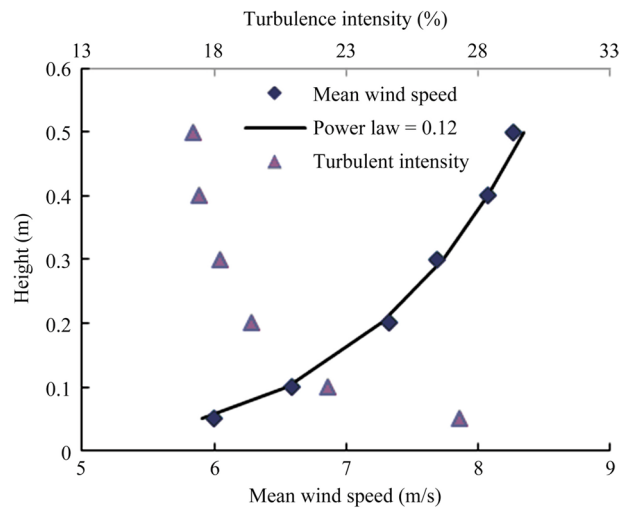


Fig. 6 Mean velocity and turbulence intensity

2.3 Simulation test of wind field

To achieve a similar environment in typical mountain terrain, the wind speed is set at 12 m/s, and it can be achieved in the wind tunnel simulation of natural wind using triangular spires and floor roughness elements with a power exponent of 0.12. The wind tunnel simulation test setup and experimental models are shown in Fig. 5. The mean velocity and turbulence intensity profiles obtained from the wind speed in the wind tunnel test equipment are illustrated in Fig. 6.

2.4 Data analysis method

2.4.1 Local mean pressure coefficient

The local mean pressure coefficient measured from the physical on-scale building model is expressed in the form of a non-dimensional pressure coefficient defined as follows:

$$C_p = \frac{p_i - p_0}{\frac{1}{2} \rho U_r^2}. \tag{1}$$

Where p_0 is the static (ambient, atmospheric) reference pressure, which is chosen from the reference height at 1 m in the wind tunnel test experiment, and the reference height at 1 m is equivalent to an actual height of 40 m above the ground; p_i is instantaneous surface pressure; ρ is the air density; U_r means the velocity measured at the reference height of the model.

2.4.2 Shape coefficient

The local mean shape coefficient is the i -th pressure tap testing point on the structure surface, which can be obtained from the following formula. According to “Load code for the design of building structures (GB 50009–2012)”, the global shape coefficient can be changed as the local shape coefficient from the following formula:

$$\overline{\mu_{si}} = \overline{C_{pi}} \left(\frac{z_r}{z_i} \right)^{2\alpha}. \tag{2}$$

Where α is the roughness index of the ground; z_i is the height of the measurement point; z_r is the height of the reference point.

The formula (2) has its truncation height, which is 5 m, and belongs to the typical mountain terrain classification A. If the height of the pressure tap testing points is below 5 m, it is not suitable to use the formula (2). Some appropriate modifications need to be made.

The shape coefficient of the surface of the structure can be obtained by the following formula:

$$\mu_s = \frac{\sum_i \overline{\mu_{si}} A_i}{A}. \tag{3}$$

Where A_i is the area of the pressure tap testing point; A is the total surface area.

2.4.3 Influence factor

To understand the overall impact of slope on low-rise buildings, a contrastive analysis of the influence factor (IF), namely the shape coefficients of all surfaces (under different slope-height conditions), can be expressed below:

$$IF = \frac{\mu_I - \mu_A}{|\mu_A|} \times 100\%. \tag{4}$$

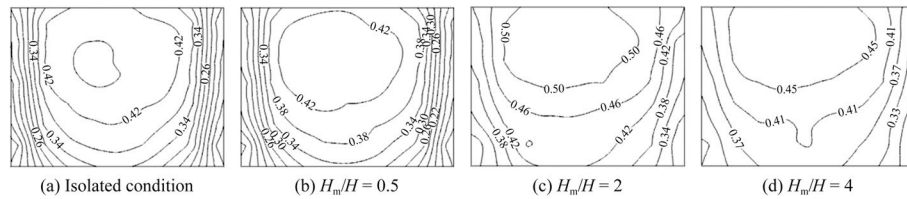


Fig. 7 Windward's contour curves of mean wind pressures

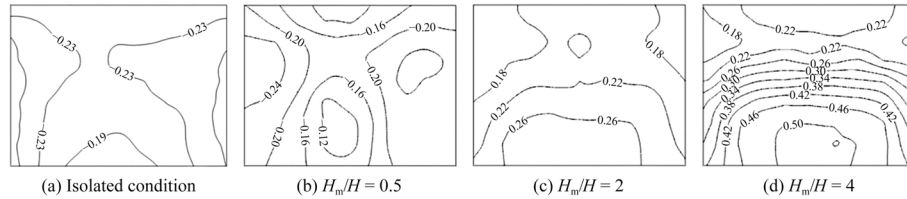


Fig. 8 Leeward's contour curves of mean wind pressures

Where μ_l is the shape coefficient under the mountain condition; μ_A is the shape coefficient without the surrounding condition.

3 Analysis of the effect of the slopes' influence under a wind attack angle of 0°

3.1 Analysis of distribution patterns of wind pressure on surfaces

The contour maps show the mean wind pressure coefficients of points on the surface under four conditions: isolated condition; $H_m/H = 0.5, 2,$ and 4 . The numerical difference between every two adjacent contours is 0.04 .

As shown in Fig. 7a, the mean wind pressure coefficients of points on the windward surface of the low-rise building model in the isolated condition are all positive. The maximum pressure on the central area is at a height of $2/3$ of the height of the physical on-scale building model. An airflow stagnation area is formed in this windward area, with a low wind speed and the highest pressure. The wind pressure coefficients of pressure tap testing points on this stagnation area are around 0.42 , and the stagnated airflow spreads from this area to the periphery with weaker and weaker effects. In the condition of $H_m/H = 0.5$ (Fig. 7b), the distribution of the wind pressure coefficients of pressure tap testing points on the windward surface is almost the same as that under the isolated condition. In other words, the slope does not influence the wind pressure distribution of the upstream physical on-scale building model. In the condition of $H_m/H = 2$ (Fig. 7c), compared with condition (b) (Fig. 7b), the mean wind pressure coefficients of pressure tap testing points on the windward surface increase slightly. In the condition of $H_m/H = 4$ (Fig. 7d), the mean wind pressure coefficients about pressure tap testing points on the windward surface decrease. It is easy to find out the mean wind pressures of windward reach their maximum value.

As shown in Fig. 8, the contours of wind pressure coefficients at the left and right sides of the leeward surface are sunken towards the center. Part of the airflow, blocked by the physical on-scale building model, bypasses the model, flows into the back, and forms a pair of vertical vortexes in opposite directions at the left and right sides of the leeward surface. The contours of wind pressure coefficients at the upper and lower

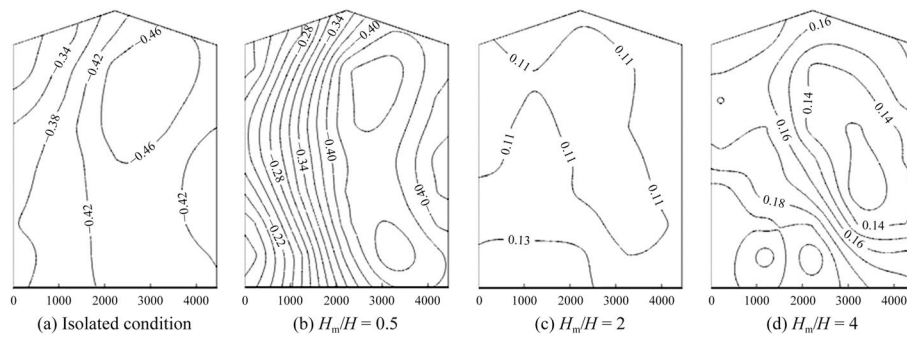


Fig. 9 Flank’s contour curves of mean wind pressures

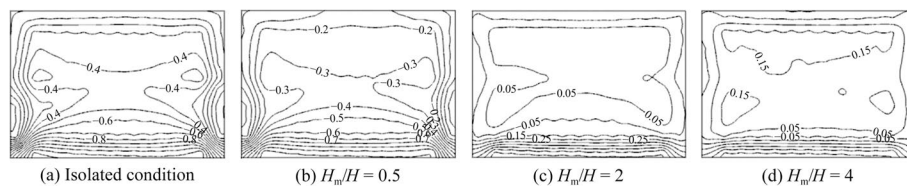


Fig. 10 Roof’s contour curves of mean wind pressures

sides of the leeward surface are sunken towards the center as well, and this is because vortexes are formed at both upper and lower sides of the leeward surface, with the upper one caused by the airflow separated by the eave and the lower one caused by the circulation formed by the shear layer on the surface. In the isolated condition (Fig. 8a), the mean wind pressure coefficients of points on the leeward surface have no significant difference from that under the condition of Fig. 8b and the coefficients under both conditions are negative, and the surface is subjected to suction. With the increase of H_m , the wind pressure on the leeward surface turns from negative to positive under the conditions of Fig. 8c and d; the mean wind pressure coefficients of pressure tap testing points on some area reach 0.5, and the wind pressure coefficients go up with the increase of the slope height. Thus, the influence of interfering slopes shall be fully considered in wind-resistant design.

As shown in Fig. 9, the distributions of wind pressure on the two flanks are symmetrical for each other, so the following analysis is made for the flank selected at random. It can be found from Fig. 9, under the condition of $H_m/H=0.5$ (Fig. 9b), the mean wind pressure coefficients of pressure tap testing points on the flank close to the windward surface are similar to that under the isolated condition (Fig. 9a), with both of the coefficients around -0.4 , and the absolute value of the coefficients under both the conditions decrease along the wind direction. In addition, the wind pressure coefficients of pressure tap testing points on the other area of the flank decrease even more than the wind pressure coefficients under the condition of $H_m/H=0.5$ (Fig. 9b). The negative wind pressure on some parts of the flank weakens when there is a slope behind the building model. From Fig. 9c and d, when the H_m is two times and four times the height of H , the wind pressure coefficients under these two conditions both are positive and the absolute values are nearly the same, all belonging to the interval of $(0.1, 0.2)$. Also, the wind pressure coefficients change from the peak value, -0.46 to 0.15 when there is a slope behind the

physical on-scale building model and $H_m/H \geq 2$. That means a low-rise building in front of a mountain is good for the flanks to resist wind.

In the isolated condition (Fig. 10a), the mean wind pressure on the roof behaves as a suction. When there is a slope behind the physical on-scale building model and $H_m/H = 0.5$ (Fig. 10b), the absolute values of mean wind pressure coefficients of pressure tap testing points on the roof decline somewhat in comparison with the isolated condition (Fig. 10a). Under the condition of $H_m/H = 2$ (Fig. 10c), except the mean wind pressure coefficients of points on the front edge, which are negative, all other mean wind pressure coefficients are small positive, 0.05, representing little mean wind pressure. Under the condition of $H_m/H = 4$ (Fig. 10d), the mean wind pressure on the front edge is very slight, and the pressure on the other part increases with the slope height, with the wind pressure coefficients reaching 0.15.

In conclusion, when there is a slope behind the low-rise building, with the H_m/H increasing from 0.5 to 4, the mean wind pressure coefficients of pressure tap testing points on the front edge decrease, and the negative pressure on this area weakens as well; the negative pressure on the other part weakens gradually and turns to positive pressure. This shows that the slope has a significant influence on the wind pressure on the roof, and with the increase of the slope height, the wind pressure gradually turns to positive pressure from negative pressure.

3.2 Wind pressure coefficients and key representative pressure tap testing points

As shown in Fig. 11, the representative pressure tap testing points are selected from the roof centerline and all four walls of the physical on-scale building model. A

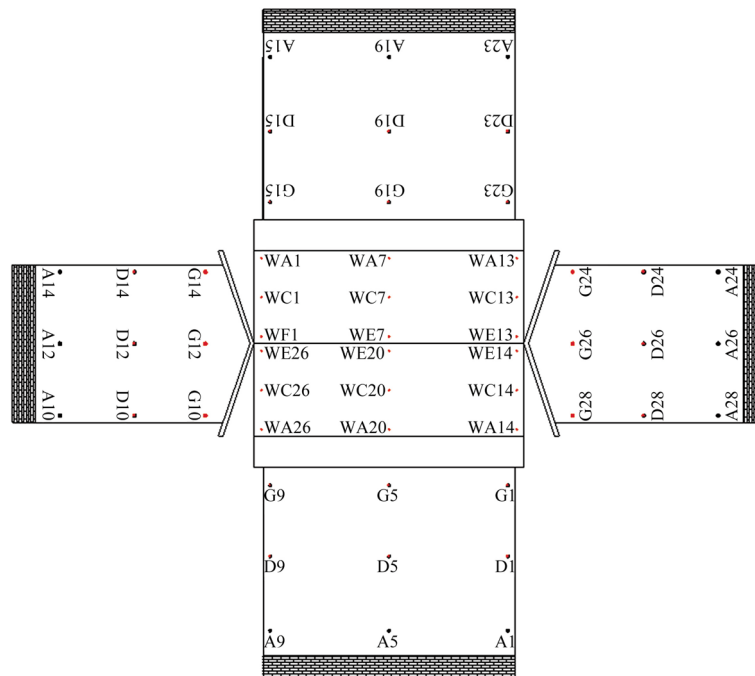


Fig. 11 Locations of representative pressure taps

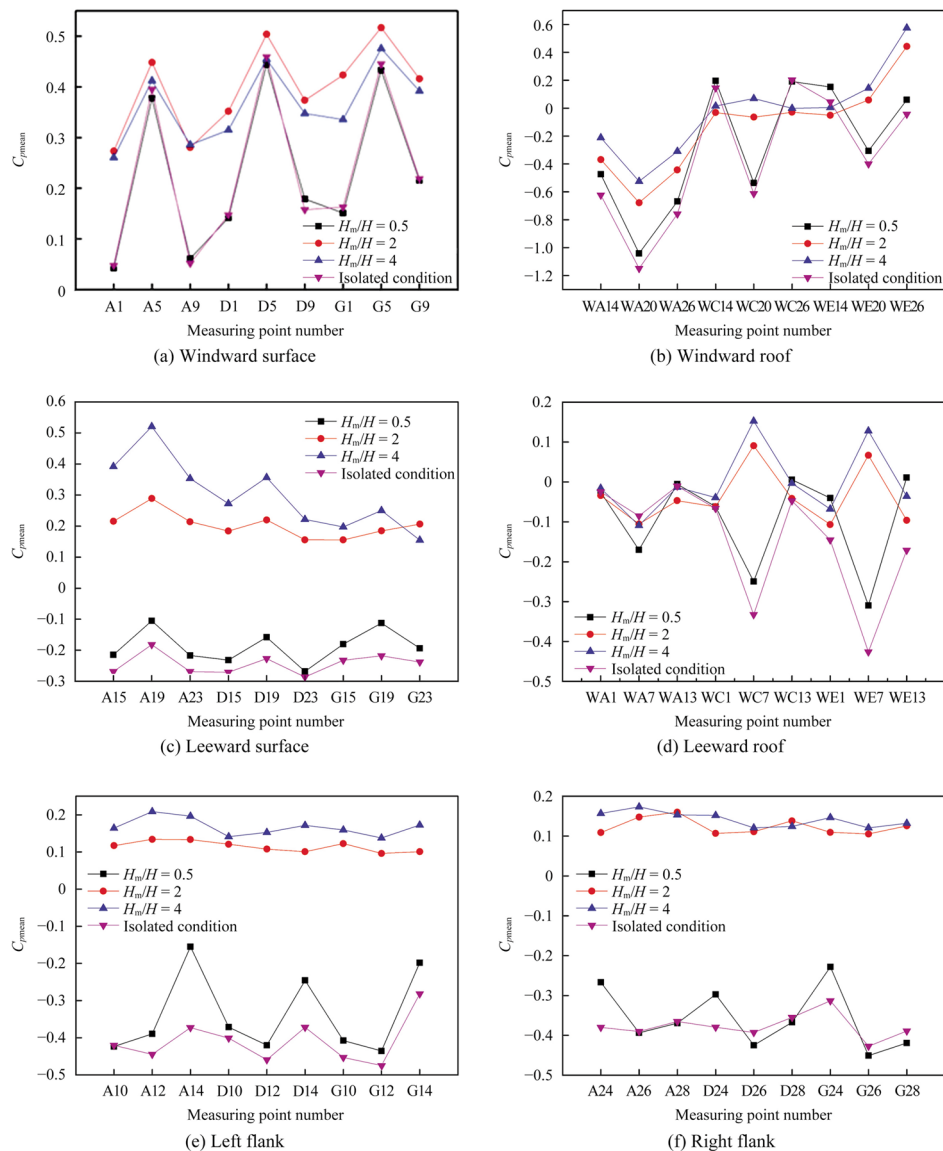


Fig. 12 Mean wind pressure coefficient of representative pressure taps in different cases

detailed analysis of the changing rules between the mean wind pressure coefficients of the pressure tap testing points and the slope height is presented below.

In Fig. 12a, the mean wind pressure coefficients of the measuring points on the centerline concerning the windward surface, A5, D5, and G5, are smaller when affected by a slope than under the isolated condition, and tend to be larger when the pressure tap testing points are on the sidewalls. In the condition of $H_m/H = 0.5$, the mean wind pressure coefficient of A5 is 744% larger than the mean wind pressure present in A1. Under the conditions of $H_m/H = 2$ and 4, the mean wind pressure coefficients of the pressure tap testing points on the sidewall are higher than the values of the isolated condition, and the mean wind pressure coefficients under the condition of $H_m/H = 0.5$ are smaller than the isolated condition. The mean wind pressure coefficients of

A9 and D9 under the condition of $H_m/H = 0.5$ show a trend close to the isolated condition.

From Fig. 12b, in the isolated condition and the condition of $H_m/H = 0.5$, the mean wind pressure coefficients of the pressure taps on the roof centerline of the windward roof, WA20, WC20, and WE20, are smaller than those of the measuring points on the sidelines. In the isolated condition, the absolute value of the mean wind pressure coefficient is WA20, which is 170.8% larger than WA14. In the isolated condition, the mean wind pressure coefficients of WC14 and WC26 (on the roof centerline of the windward roof) and WE14 (on the ridge line) are higher than those under the slope-interfering conditions, and the mean wind pressure coefficients of other pressure tap testing points are lower than those under the slope-interfering conditions. The mean wind pressure coefficients of WC20 and WC26 under the condition of $H_m/H = 0.5$ are very close to the isolated condition.

From Fig. 12c, the mean wind pressure coefficients of the pressure taps on the leeward surface under the condition of $H_m/H = 0.5$ are close to those under the isolated condition, and the mean wind pressure coefficients under the condition of $H_m/H = 2$ are close to those under the condition of $H_m/H = 4$. The absolute values of mean wind pressure coefficients of the pressure testing points on the roof centerline are higher than the absolute values on the sidewall, and the coefficients are positive. The absolute values of the pressure tap testing points on the roof centerline are smaller than those on the sidelines in case the coefficients are negative. In the isolated condition, the absolute value of the mean wind pressure coefficient of A19 decrease by 25.9% compared with that of A15, and in the condition of $H_m/H = 4$, the mean wind pressure coefficient of A19 increases by 37.5% compared with that of A15.

In Fig. 12d, the smallest absolute value of the mean wind pressure coefficient of WA7 (the intermediate measuring point on the leeward eave) is reached under the isolated condition. WC7 (the intermediate measuring point on the leeward roof) and WE7 (the middle measuring point on the leeward ridge) are significantly influenced by the slope, and the mean wind pressure coefficients under these two conditions turn from negative to positive with an increase of H_m/H . When H_m/H increases from 2 to 4, the mean wind pressure coefficients have a larger increase. In the isolated condition, the absolute value of the mean wind pressure coefficient of WE7 increases by 166.7% compared with the mean wind pressure coefficient of WE1.

As shown in Fig. 12e and f, the mean wind pressure coefficients of A14, D14, and G14 (the measuring points on the left sideline of the left flank), A24, D24, and G24 (the measuring points on the right sideline of the right flank) are higher than other points. In the condition of $H_m/H = 0.5$, the absolute value of the mean wind pressure coefficient of A14 (the measuring point on the left sideline of the left flank) decreases by 60.5% compared with the absolute value of the mean wind pressure coefficient of A10 (the middle point), and the absolute value of the mean wind pressure coefficient of G24 (the measuring point on the right sideline of the right flank) decreases by 53.3% compared with the absolute value of the mean wind pressure coefficient of G26 (the middle point). The mean wind pressure coefficients of pressure tap testing points on the left and right flanks under the condition of $H_m/H = 0.5$ are close to the isolated

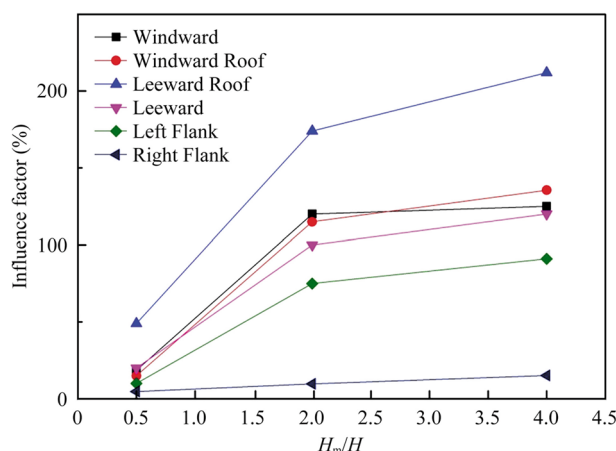


Fig. 13 Influence coefficient

condition, and the mean wind pressure coefficients under the condition of $H_m/H = 2$ are close to the condition of $H_m/H = 4$.

3.3 Analysis of changing rules of shape coefficients

To understand the overall impact of slope on low-rise buildings, a contrastive analysis of the influence factor (IFs) is made. The shape coefficient of all four surfaces (see the formula (4)) under different slope-height conditions is selected. Figure 13 shows the changing rules of IFs under the conditions of $H_m/H = 0.5, 2$, and 4 , with a wind angle of 0° and a slope angle $\beta = 60^\circ$.

Also, it is shown that under the condition of $H_m/H = 0.5$, the overall influence of the slope on each surface is small, with IFs less than 50%. However, IFs increase with the increase of the slope height. IFs of the windward surface under the condition of $H_m/H = 2$ are close to those under the condition of $H_m/H = 4$. Under the condition of $H_m/H = 4$, IFs reach the maximum number for each surface, with the leeward roof having the highest IFs; the surfaces' IFs are in descending order from 213%, 148%, 125%, 120%, 87%, to 20%, which are respectively for the leeward roof, windward roof, windward surface, leeward surface, left flank, and right flank.

4 Analysis of the effect of slopes with different wind angles

To find out the changes of mean wind pressure coefficients of pressure tap testing points on surfaces with a wind angle, D5 (the central point on the windward surface), D12 (the central point on the flank), D19 (the central point on the leeward surface), WA20 (the middle point on the windward eave), and WA7 (the intermediate point on the leeward eave) are selected, and the changing rules of mean wind pressure coefficients of points on the surfaces with a wind angle are analyzed under different conditions. The results are shown in Fig. 14.

As shown in Fig. 14, the mean wind pressure coefficients of the pressure taps on the windward surface gradually decrease with increasing wind angle under all the conditions. Compared with the isolated condition, all other conditions have higher decrease rates. The mean wind pressure coefficient of the pressure tap testing point on the

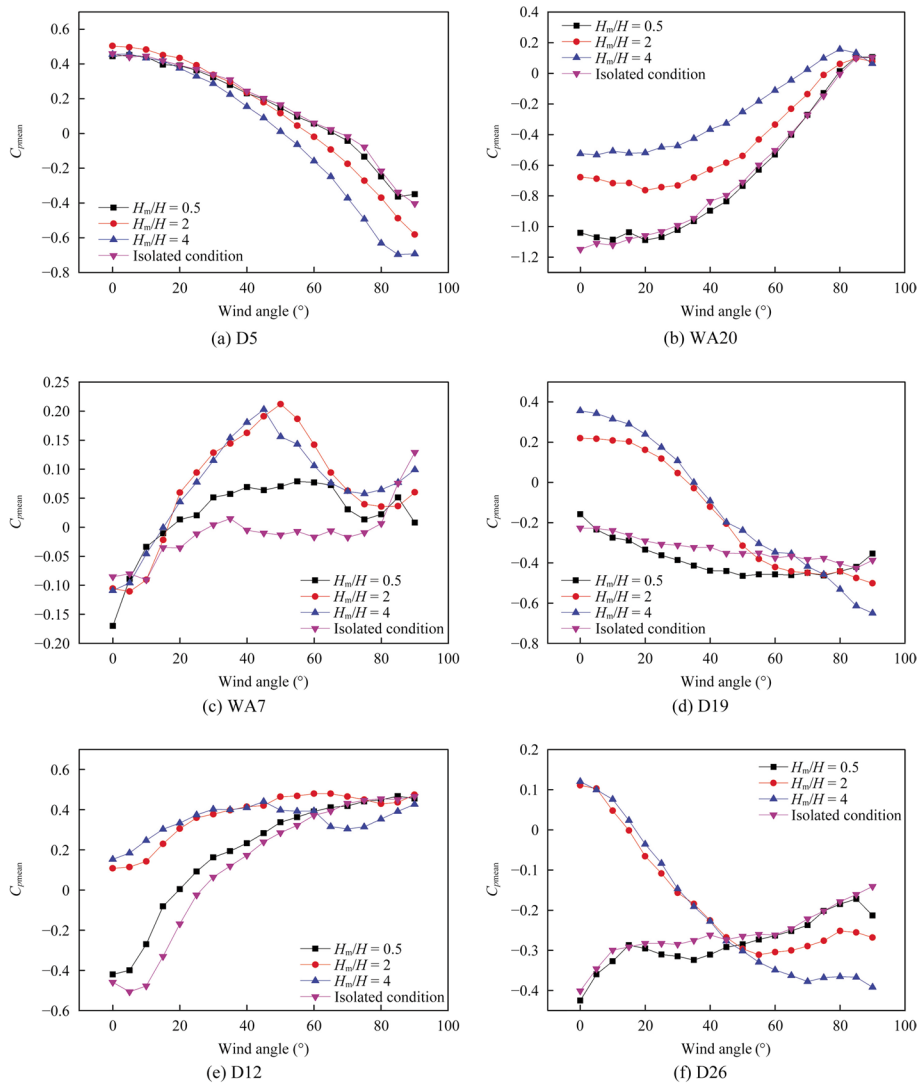


Fig. 14 Mean wind pressure coefficient of representative pressure taps in different wind angles

windward surface does not change significantly with the slope height change. When the wind angle is within $0^\circ - 40^\circ$, the mean wind pressure coefficient under the isolated condition is close to that in the condition of $H_m/H=0.5$, and the value under the condition of $H_m/H=2$ is close to that in the condition of $H_m/H=4$. When the wind angle is within $45^\circ - 90^\circ$, the mean wind pressure coefficient under the condition of $H_m/H=2$ is close to the condition of $H_m/H=4$, and the absolute value of the mean wind pressure coefficient increases with increasing H_m/H . The mean wind pressure coefficient of the pressure tap testing point on the windward eave gradually changed from negative to positive due to the increasing wind angle. Under the isolated condition, the absolute value of the mean wind pressure coefficient is higher than that under other conditions. The slope reduces the negative pressure at the pressure tap testing point on the windward eave, and the absolute value of the mean wind pressure coefficient decreases with increasing slope height.

Under the isolated condition, the mean wind pressure coefficient of the pressure tap testing point on the leeward eave changes smoothly with increasing wind angle; namely, the wind angle has little influence on it. Under other conditions, the mean wind pressure coefficient magnifies first and decreases subsequently with increasing wind angle. The maximum positive values of the mean wind pressure coefficient are observed when the wind angle is within $40^\circ - 60^\circ$. Compared with the changes of the mean wind pressure coefficients of the pressure tap testing point on the windward eave with increasing wind angle, the changes of the coefficients of the pressure tap testing point on the leeward eave are unobvious, which indicates that the wind pressure coefficients of the pressure tap testing points on the leeward roof are greatly influenced by the wind angle. In the isolated condition, the mean wind pressure coefficient of the pressure tap testing point on the leeward surface changes smoothly with the increase of the wind angle. Under the conditions affected by the slope, the mean wind pressure coefficient of the pressure tap testing point on the leeward surface changes more significantly with the wind angle, with the pressure changing from negative to positive under some conditions. In the condition of $H_m/H=2$, the mean wind pressure coefficients are close to the isolated condition, and the mean wind pressure coefficients under the condition of $H_m/H=2$ are close to the condition of $H_m/H=4$; under all the conditions, the coefficients decrease with increasing wind angle.

In the isolated condition, the mean wind pressure coefficient of the pressure tap testing point on the left flank first decreases and then increases with the increase of the wind angle. The lowest negative pressure is observed when the wind angle is 5° , and the pressure behaves as suction. After that, the mean wind pressure coefficient increases gradually with the increase of the wind angle and turns positive. Under the conditions affected by the slope, all the mean wind pressure coefficients increase compared with the isolated condition. When the wind angle is from 0° to 45° , the mean wind pressure coefficients increase with increasing wind angle. Besides, the difference between the mean wind pressure coefficients under different conditions gets smaller and smaller with increasing wind angle. When the wind angle is 90° , the mean wind pressure coefficients under each condition are close. This indicates that the slope height's influence on the mean wind pressure coefficients weakens with increasing wind angle.

When the wind angle is within $0^\circ - 45^\circ$, the mean wind pressure coefficients of the point on the right flank under the isolated condition are close to those under the condition of $H_m/H=0.5$, and the values increase with increasing wind angle. The mean wind pressure coefficients under the condition of $H_m/H=2$ are close to those under the condition of $H_m/H=4$, but the values decrease with increasing wind angle. When the wind angle is between 45° and 90° , the absolute values of the mean wind pressure coefficients decrease with decreasing slope height.

5 Summary of the variation range of zonal body type coefficient with height

From the above analysis, different areas of low-rise buildings present not-alike wind pressure distributions under different wind angles, and the leeward area, especially the leeward eave, is more significantly affected by the wind pressure. To analyze the wind pressure coefficient of different areas more systematically, the paper adopts the method of zoning the building surface to discuss the shape coefficient of different areas.

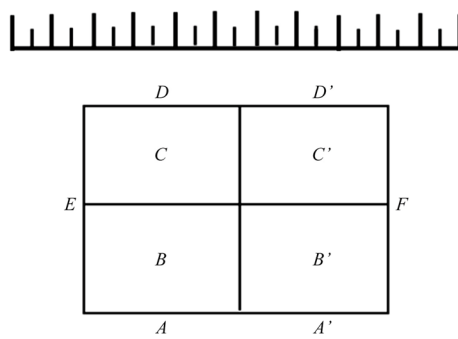


Fig. 15 Subdivision of low-rise buildings

Reference is made to the provisions of the partition division of the closed gable roof under the 90° wind direction angle in Article 24 of Table 8.3.1, Section 8.3 of China’s Load code for the design of building structures, as shown in Fig. 15. This paper adopts this zoning method to summarize the variation range of body shape coefficient in different regions of the wind direction angle.

In some specific wind directions, the peak negative pressure at the airflow separation increases significantly. It is extremely unfavorable to wind resistance. The distribution law of surface wind pressure of each body shape coefficient of low-rise buildings under the combination of $H_m/H=0.5, 2.0,$ and 4.0 with wind angles ranging from 0° to 90° is summarized in Table 2 (α indicates the corresponding wind direction when the absolute value of the body shape coefficient is maximum), which provides a reference for the design of low-rise buildings in the future.

6 Conclusions

Through the wind tunnel tests for the physical on-scale low-rise building model in three typical offshore mountain landscapes, this paper mainly discusses the distribution patterns of pressure on the surfaces of low-rise buildings under the influence of slopes with different heights. The conclusions are summarized as follows.

1. The mean wind pressure coefficients of pressure taps on all the surfaces under the condition of $H_m/H=0.5$ are close to those under the isolated condition. The mean wind pressure of the windward has the maximum value when $H_m/H=2$. In both $H_m/H=2$ and $H_m/H=4$, the mean wind pressure value on the leeward surface turns from negative to positive, and the mean wind pressure coefficients increase when the slope height increases; the negative mean wind pressure on some parts of the flanks weakens, and on the roof also turns from negative to positive. The slope’s height influences the mean wind pressure on the roof, so the impact of interfering slopes shall be fully considered in the wind-resistant design.
2. Some pressure tap testing points, including WA20 (the middle point on the windward eave) and WE7 (the middle point on the leeward ridge), are under high negative mean wind pressure in the isolated condition. The mean wind pressure coefficient values of A5, D5, and G5 (points on the center line of the windward surface), A19, D19, and G19 (points on the center line of the leeward surface) are higher than the pressure tap testing points on the sidelines; the mean wind pressure coefficient

Table 2 Variation range of body shape coefficient at different wind angles

H_m/H	A			B			C			D			A'		
	Range of variation	α	Range of variation	Range of variation	α	Range of variation	Range of variation	α	Range of variation	Range of variation	α	Range of variation	Range of variation	α	Range of variation
0.5	(0.77, 0.63)	85°	(-0.73, -0.33)	85°	35°	(-1.03, -0.29)	(-0.95, -0.08)	35°	(-0.47, 0.57)	90°	(-0.74, 0.69)	(-1.20, 0.79)	90°	(-0.60, 0.01)	90°
2.0	(1.0, 0.73)	80°	(-1.01, 0.39)	90°	90°	(-1.04, 0.42)	(-1.08, 0.67)	90°	(-0.74, 0.69)	90°	(-1.08, 0.67)	(-1.20, 0.79)	90°	(-0.67, 0.27)	90°
4.0	(1.62, 0.83)	75°	(-1.46, 0.69)	85°	75°	(-1.50, 0.68)	(-1.62, 0.79)	75°	(-1.20, 0.79)	90°	(-1.62, 0.79)	(-1.20, 0.79)	70°	(-1.03, 0.47)	90°
		B'		C'			D'		E		F				
		Range of variation		Range of variation		Range of variation	Range of variation		Range of variation		Range of variation		Range of variation		Range of variation
H_m/H	0.5	(-0.65, 0.03)	α	(-0.62, 0)	α	(-0.68, -0.07)	(-0.67, 0.54)	α	(-0.60, 0.01)	α	(-0.67, 0.54)	(-0.67, 0.54)	α	(-0.60, 0.01)	α
	2.0	(-0.54, 0.33)	15°	(-0.64, 0.39)	40°	(-0.82, 0.62)	(-0.44, 0.66)	45°	(-0.67, 0.27)	55°	(-0.44, 0.66)	(-0.44, 0.66)	50°	(-0.67, 0.27)	55°
	4.0	(-0.79, 0.64)	35°	(-0.80, 0.66)	85°	(-1.14, 0.72)	(-0.43, 0.86)	85°	(-1.14, 0.72)	60°	(-0.43, 0.86)	(-0.43, 0.86)	5°	(-1.03, 0.47)	80°

value of A19 reaches around 0.56 when $H_m/H=4$. Concerning all the above pressure tap testing points with relatively high partial wind pressure, the partial wind pressure coefficients can be introduced in the design to avoid partial damage to houses.

3. The slope's overall influence on all the surfaces is relatively small, with IFs less than 50% in $H_m/H=0.5$. Increasing the slope height comes with increasing IFs. IFs of the windward surface of $H_m/H=2$ are close to those of $H_m/H=4$. When $H_m/H=4$, IFs reach the maximum for each surface, with the leeward roof having the highest IFs; the IFs of the surface are in descending order, 213%, 148%, 125%, 120%, 87%, and 20%, respectively for the leeward roof, windward roof, windward surface, leeward surface, left flank, and right flank.
4. At different wind angles, the distribution pattern of the mean wind pressure coefficients of pressure tap testing points on the center lines of the leeward surface and the right flank in the isolated conditions is significantly different from that under the conditions affected by slopes. With the increase of the hillside's height, the changing trend of the mean wind pressure coefficients of pressure tap testing points on each surface is different. The mean wind pressure coefficient is influenced by the wind angle. When the wind angle is 0° , under the isolated condition, the negative peak value (-1.15) of the mean wind pressure coefficient is observed at the middle point on the windward eave. Therefore, the wind load at the wind angle producing the most negative effect shall be considered during the calculation when designing low-rise buildings in typical mountain terrain areas.

Acknowledgements

Not applicable.

Authors' contributions

MZ, FX, ZZ, and ZL made substantial contributions to the conception; MZ, JL, and ML made substantial contributions to the design of the work, and the acquisition, analysis, and interpretation of data. ML and JL made substantial contributions to draft the work. MZ, ZZ, and ZL revised the manuscript. The authors read and approved the final manuscript.

Funding

The work described in this paper was supported by the Science Research Project of the Hebei Education Department (BJ2020010) and the National Natural Science Foundation Of China (51478179, 51178180).

Availability of data and materials

The datasets used and analyzed during the current study are available from the Key Laboratory of Building Safety and Energy Efficiency (Hunan University), Ministry of Education.

Declarations

Competing interests

The authors declare that they have no competing interests.

Received: 12 September 2023 Accepted: 31 January 2024

Published online: 01 April 2024

References

1. John AD, Gairola A, Mukherjee M (2009) Interference effect of boundary wall on wind loads. Paper presented at the 11th American conference on wind engineering, San Juan, 13-18 June 2009
2. Lien FS, Yee E, Cheng Y (2004) Simulation of mean flow and turbulence over a 2D building array using high-resolution CFD and a distributed drag force approach. *J Wind Eng Ind Aerod* 92(2):117–158
3. Zhang A, Gao C, Zhang L (2005) Numerical simulation of the wind field around different building arrangements. *J Wind Eng Ind Aerod* 93(12):891–904
4. Holmes JD (1994) Wind pressures on tropical housing. *J Wind Eng Ind Aerod* 53(1–2):105–123

5. Pindado S, Meseguer J, Franchini S (2011) Influence of an upstream building on the wind-induced mean suction on the flat roof of a low-rise building. *J Wind Eng Ind Aerod* 99(8):889–893
6. Tsutsumi J, Katayama T, Nishida M (1992) Wind tunnel tests of wind pressure on regularly aligned buildings. *J Wind Eng Ind Aerod* 43(1–3):1799–1810
7. Kim YC, Yoshida A, Tamura Y (2012) Characteristics of surface wind pressures on low-rise building located among large group of surrounding buildings. *Eng Struct* 35:18–28
8. Chang CH, Meroney RN (2003) The effect of surroundings with different separation distances on surface pressures on low-rise buildings. *J Wind Eng Ind Aerod* 91(8):1039–1050
9. Kim YC, Yoshida A, Tamura Y (2013) Influence of surrounding buildings on wind loads acting on low-rise building. *J Struct Eng* 139(2):275–283
10. Mostafa K, Zisis I, Stathopoulos T (2022) Large-scale wind testing on roof overhangs for a low-rise building. *J Struct Eng* 148(11):04022173
11. Kopp GA, Wu CH (2020) A framework to compare wind loads on low-rise buildings in tornadoes and atmospheric boundary layers. *J Wind Eng Ind Aerod* 204:104269
12. Zhong M, Li Z, Qiu M et al (2016) Wind tunnel test on wind load of low-rise buildings in typical mountain landform: analysis of hillside slope effects. *Acta Aerodyn Sin* 34(5):687–695
13. Zhong M (2018) Wind-resistant performance study on low-rise building in typical mountain terrain. Dissertation, Hunan University

Publisher's Note

Springer Nature remains neutral with regard to jurisdictional claims in published maps and institutional affiliations.